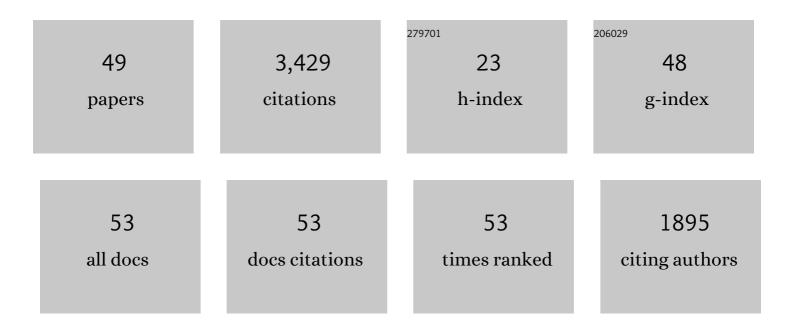


## List of Publications by Year in descending order

Source: https://exaly.com/author-pdf/3575425/publications.pdf Version: 2024-02-01



#	Article	IF	CITATIONS
1	Defects and anomalies in powder bed fusion metal additive manufacturing. Current Opinion in Solid State and Materials Science, 2022, 26, 100974.	5.6	157
2	The interplay between vapour, liquid, and solid phases in laser powder bed fusion. Nature Communications, 2022, 13, .	5.8	30
3	In Situ Analysis of Laser Powder Bed Fusion Using Simultaneous High-Speed Infrared and X-ray Imaging. Jom, 2021, 73, 201-211.	0.9	51
4	High-speed synchrotron X-ray imaging of directed energy deposition of titanium: effects of processing parameters on the formation of entrapped-gas pores. Procedia Manufacturing, 2021, 53, 148-154.	1.9	3
5	Universal scaling laws of keyhole stability and porosity in 3D printing of metals. Nature Communications, 2021, 12, 2379.	5.8	105
6	Solidification crack propagation and morphology dependence on processing parameters in AA6061 from ultra-high-speed x-ray visualization. Additive Manufacturing, 2021, 42, 101959.	1.7	12
7	The causal relationship between melt pool geometry and energy absorption measured in real time during laser-based manufacturing. Applied Materials Today, 2021, 23, 101049.	2.3	28
8	In situ X-ray imaging of pore formation mechanisms and dynamics in laser powder-blown directed energy deposition additive manufacturing. International Journal of Machine Tools and Manufacture, 2021, 166, 103743.	6.2	58
9	<i>In situ</i> characterization of laser-generated melt pools using synchronized ultrasound and high-speed X-ray imaging. Journal of the Acoustical Society of America, 2021, 150, 2409-2420.	0.5	16
10	Time-Resolved Geometric Feature Tracking Elucidates Laser-Induced Keyhole Dynamics. Integrating Materials and Manufacturing Innovation, 2021, 10, 677-688.	1.2	4
11	In-situ full-field mapping of melt flow dynamics in laser metal additive manufacturing. Additive Manufacturing, 2020, 31, 100939.	1.7	69
12	Critical instability at moving keyhole tip generates porosity in laser melting. Science, 2020, 370, 1080-1086.	6.0	316
13	Laser powder bed fusion of Inconel 718 on 316 stainless steel. Additive Manufacturing, 2020, 36, 101500.	1.7	9
14	Simultaneous high-speed x-ray transmission imaging and absolute dynamic absorptance measurements during high-power laser-metal processing. Procedia CIRP, 2020, 94, 775-779.	1.0	15
15	Revealing transient powder-gas interaction in laser powder bed fusion process through multi-physics modeling and high-speed synchrotron x-ray imaging. Additive Manufacturing, 2020, 35, 101362.	1.7	20
16	Types of spatter and their features and formation mechanisms in laser powder bed fusion additive manufacturing process. Additive Manufacturing, 2020, 36, 101438.	1.7	48
17	Direct observation of pore formation mechanisms during LPBF additive manufacturing process and high energy density laser welding. International Journal of Machine Tools and Manufacture, 2020, 153, 103555.	6.2	143
18	Preliminary Study on the Influence of an External Magnetic Field on Melt Pool Behavior in Laser Melting of 4140 Steel Using In-Situ X-Ray Imaging. Journal of Micro and Nano-Manufacturing, 2020, 8, .	0.8	6

CANG ZHAO

#	Article	IF	CITATIONS
19	In situ Characterization of Laser Powder Bed Fusion Using High-Speed Synchrotron X-ray Imaging Technique. Microscopy and Microanalysis, 2019, 25, 2566-2567.	0.2	2
20	Pore elimination mechanisms during 3D printing of metals. Nature Communications, 2019, 10, 3088.	5.8	158
21	In-situ high-speed X-ray imaging of piezo-driven directed energy deposition additive manufacturing. Scientific Reports, 2019, 9, 962.	1.6	96
22	Bulk-Explosion-Induced Metal Spattering During Laser Processing. Physical Review X, 2019, 9, .	2.8	34
23	Effect of Laser-Matter Interaction on Molten Pool Flow and Keyhole Dynamics. Physical Review Applied, 2019, 11, .	1.5	107
24	In-situ characterization and quantification of melt pool variation under constant input energy density in laser powder bed fusion additive manufacturing process. Additive Manufacturing, 2019, 28, 600-609.	1.7	103
25	In situ synchrotron X-ray imaging of 4140 steel laser powder bed fusion. Materialia, 2019, 6, 100306.	1.3	52
26	High-speed Synchrotron X-ray Imaging of Laser Powder Bed Fusion Process. Synchrotron Radiation News, 2019, 32, 4-8.	0.2	17
27	Investigating Powder Spreading Dynamics in Additive Manufacturing Processes by <i>In-situ</i> High-speed X-ray Imaging. Synchrotron Radiation News, 2019, 32, 9-13.	0.2	16
28	In Situ Characterization of Hot Cracking Using Dynamic X-Ray Radiography. Minerals, Metals and Materials Series, 2019, , 77-85.	0.3	6
29	Real time observation of binder jetting printing process using high-speed X-ray imaging. Scientific Reports, 2019, 9, 2499.	1.6	88
30	Keyhole threshold and morphology in laser melting revealed by ultrahigh-speed x-ray imaging. Science, 2019, 363, 849-852.	6.0	592
31	Transient dynamics of powder spattering in laser powder bed fusion additive manufacturing process revealed by in-situ high-speed high-energy x-ray imaging. Acta Materialia, 2018, 151, 169-180.	3.8	276
32	Crushing of circular steel tubes filled with nanoporous-materials-functionalized liquid. International Journal of Damage Mechanics, 2018, 27, 439-450.	2.4	12
33	Revealing particle-scale powder spreading dynamics in powder-bed-based additive manufacturing process by high-speed x-ray imaging. Scientific Reports, 2018, 8, 15079.	1.6	85
34	Ultrafast X-ray imaging of laser–metal additive manufacturing processes. Journal of Synchrotron Radiation, 2018, 25, 1467-1477.	1.0	142
35	Effects of porosity on dynamic indentation resistance of silica nanofoam. Scientific Reports, 2017, 7, 1060.	1.6	0
36	Enhanced resistance of nanocellular silica to dynamic indentation. Materials Science & Engineering A: Structural Materials: Properties, Microstructure and Processing, 2017, 693, 121-128.	2.6	0

CANG ZHAO

#	Article	IF	CITATIONS
37	Real-time monitoring of laser powder bed fusion process using high-speed X-ray imaging and diffraction. Scientific Reports, 2017, 7, 3602.	1.6	389
38	Variation of microstructure and mechanical properties of medium Mn steels with multiphase microstructure. Materials Science and Technology, 2016, 32, 63-70.	0.8	4
39	Fast-condensing nanofoams: Suppressing localization of intense stress waves. Materials Science & Engineering A: Structural Materials: Properties, Microstructure and Processing, 2016, 676, 450-462.	2.6	4
40	Characterization of nanoporous structures: from three dimensions to two dimensions. Nanoscale, 2016, 8, 17658-17664.	2.8	18
41	High-temperature post-processing treatment of silica nanofoams of controlled pore sizes and porosities. Materials and Design, 2016, 90, 815-819.	3.3	8
42	Inorganic–Organic Hybrid of Lunar Soil Simulant and Polyethylene. Journal of Materials in Civil Engineering, 2016, 28, .	1.3	13
43	Appropriate Osmotic Balance Duration for Different Volumes of Ovarian Tissue in Vitrification Solution: a Study of Ovary Tissue Vitrification and Transplantation in Sheep. Cryo-Letters, 2016, 37, 365-378.	0.1	0
44	Non-dissipative energy capture of confined liquid in nanopores. Applied Physics Letters, 2014, 104, 203107.	1.5	21
45	Performance of thermally-chargeable supercapacitors in different solvents. Physical Chemistry Chemical Physics, 2014, 16, 12728-12730.	1.3	17
46	Effect of annealing temperature and time on microstructure evolution of 0·2C–5Mn steel during intercritical annealing process. Materials Science and Technology, 2014, 30, 791-799.	0.8	23
47	Modified infiltration of solvated ions and ionic liquid in a nanoporous carbon. Applied Physics A: Materials Science and Processing, 2013, 112, 885-889.	1.1	7
48	Effects of molecular polarity on nanofluidic behavior in a silicalite. International Journal of Materials Research, 2013, 104, 594-597.	0.1	2
49	New Jamming Scenario: From Marginal Jamming to Deep Jamming. Physical Review Letters, 2011, 106, 125503.	2.9	44